View metadata, citation and similar papers at core.ac.uk
brought to you by CORE
provided by Agder University Research Archive

Performance Analysis of Alamouti Coded OFDM Systems over Rayleigh Fading Channels Correlated in Space and Time

Yuanyuan Ma and Matthias Pätzold
University of Agder
Servicebox 509, NO-4898, Grimstad, Norway
E-mails: {yuanyuan.ma, matthias.paetzold}@uia.no

***Abstract*—This paper deals with the performance analysis of Alamouti coded orthogonal frequency division multiplexing (OFDM) systems over time-varying multipath Rayleigh fading channels. In our analysis, we consider a physically more realistic channel, which can be correlated either in time or in space or even in both domains. We derive an analytical expression for the bit error probability (BEP), which describes the performance of an Alamouti coded OFDM system over fading channels correlated in space and time. It is shown that the derived BEP can be reduced to the known BEP obtained over fading channels correlated in time or space. The correctness of all theoretical results is validated by system simulations. The knowledge of the obtained theoretical results makes the BEP evaluation more straightforward and less time-consuming compared to simulations. Moreover, it allows us to discuss the effect of the maximum Doppler frequency and the antenna spacing on the system performance.**

I. Introduction

In the past two decades, space-time block coding (STBC) schemes have received considerable attention due to the fact that they can increase the transmission reliability over wireless fading channels [1]. One of the famous and simple STBCs is the Alamouti coding scheme [2], which has been proposed by Alamouti to achieve a transmit diversity gain. It has been shown in the literature, e.g., in [3], that the simple Alamouti scheme works well if the mobile fading channel remains constant over an Alamouti codeword period. Due to the increasing demand for high data rate wireless communication services, future communication systems are supposed to be operating in much larger bandwidth ranges than today's communication systems. To cope with the multipath fading problem faced by future wideband communication systems, one efficient solution is to combine the Alamouti scheme with OFDM techniques.

Since the symbol duration of an OFDM system is much longer than that of a single-carrier system, a channel which is quasi-static for a single-carrier system may not be quasi-static for an OFDM system. Therefore, when studying the performance of an Alamouti coded OFDM system, it is physically not realistic to consider the channel as time invariant over two consecutive symbol durations. The impact of a time-varying fading channel on the performance of Alamouti coded OFDM systems has been investigated in [4]. The drawback of this paper is that the spatial correlation between the Rayleigh fading subchannels has not been taken into account. However, it has been shown in [5] by simulations and in [6] by theory that the performance of an Alamouti coded OFDM system depends not only on the temporal correlation but also on the spatial correlation. Due to this fact, the authors in [7] have studied the impact of both the temporal and the spatial properties on the performance of Alamouti coded OFDM systems. However, in [7], the authors assumed that the subchannels cannot be correlated simultaneously in time and space. For example, they assumed that no spatial correlation exists when analyzing the system performance over channels correlated in time and vice versa. Thus, the results in [7] were not generally valid and they cannot be used for the realistic case where the subchannels are correlated in both time and space.

In this paper, we concentrate again on the performance analysis of Alamouti coded OFDM systems in time-varying multipath Rayleigh fading channels. In contrast to [4] and [7], we restrict our attention to the physically more realistic case that the channel can be arbitrarily correlated either in time or in space or even in both domains. In our analysis, we assume that the channel envelope changes during two consecutive transmission time slots. We derive an analytical expression for the BEP over channels correlated in space and time. We show that our derived BEP can be reduced to the BEP presented in [7] for channels correlated only in time or space. All theoretical results will be confirmed by system simulations. The obtained results allow us to study the influence of the Doppler effect and the antenna spacing on the system performance. It is shown that the system performance improvement can be achieved by increasing the antenna spacing, while the performance deteriorates if we increase the maximum Doppler frequency. It turns out that the temporal autocorrelation function (ACF) and the space cross-correlation function (CCF) have an inverse effect on the system performance though they have the same shape under isotropic scattering conditions.

The rest of the paper is organized as follows. In Section II, we briefly review the Alamouti coded OFDM system and the statistical properties of the considered wideband chan-

978-1-4244-2519-8/10/$26.00 ©2010 IEEE

nel model. Section III analyzes the BEP performance over channels correlated in space and time, where an analytical expression is derived for the BEP of Alamouti coded OFDM systems. Section IV confirms the correctness of the theory by simulation. Finally, we give the conclusions in Section V.

II. Review of The Alamouti Coded OFDM System

In this paper, we consider an OFDM system equipped with two transmit antennas and a single receive antenna. The complex data symbol pair (S_1, S_2) is encoded first by the Alamouti scheme [3] before it is transmitted over a multipath fading channel. The symbols received at the time slots t_1 and t_2 can be expressed as

$$Y_1 = H_{11}(f', x_1, t_1)S_1 + H_{21}(f', x_2, t_1)S_2 + N_1, \tag{1a}$$

$$Y_2 = -H_{11}(f', x_1, t_2)S_2^* + H_{21}(f', x_2, t_2)S_1^* + N_2, \tag{1b}$$

where N_i denotes the additive white Gaussian noise (AWGN) component at the time slot t_i $(i = 1, 2)$ and

$$H_{k1}(f', x_k, t_i) = \sum_{\ell=1}^{\mathcal{L}} a_\ell \mu_\ell(x_k, t_i) e^{-j2\pi f' \tau'_\ell} \tag{2}$$

represents the space-time-variant transfer function of the transmission link from the kth transmit antenna located at x_k $(k = 1, 2)$ to the single receive antenna. Here, $\mathcal{L}$ is the number of discrete propagation paths. The quantities a_ℓ and τ'_ℓ denote the path gain and the propagation delay of the ℓth path, respectively. It is assumed that the average power of the channel model is normalized to unity, i.e., the power constraint $\sum_{\ell=1}^{\mathcal{L}} a_\ell^2 = 1$ holds. The processes $\mu_\ell(x_k, t_i)$ in (2) represent zero-mean complex Gaussian random processes. We assume that the real and imaginary parts of $\mu_\ell(x_k, t_i)$ are uncorrelated, each having the variance $\sigma_0^2 = 1/2$.

It is supposed that the receiver knows perfectly the channel state information, and we assume that no synchronization error exists. By applying the combining strategy proposed in [8], [9], the estimated symbols at the output of the detector can be expressed in the form shown at the bottom of this page.

A. The Instantaneous Output Signal-to-Noise Ratio

For convenience, we express the complex space-time-variant transfer functions by their envelopes $R_m = |H_{k1}(f', x_k, t_i)|$ and phases $\Theta_m = \arg\{H_{k1}(f', x_k, t_i)\}$ for $m = 1, 2, 3, 4$ as follows

$$\begin{aligned} H_{11}(f', x_1, t_1) &= R_1 e^{\Theta_1}, \qquad H_{11}(f', x_1, t_2) = R_2 e^{\Theta_2}, \\ H_{21}(f', x_2, t_1) &= R_3 e^{\Theta_3}, \qquad H_{21}(f', x_2, t_2) = R_4 e^{\Theta_4}. \end{aligned} \tag{4}$$

Given the channel model described by (2), it turns out that the random envelope R_m follows the Rayleigh distribution.

Since the system model is symmetrical, the BEP of S_1 is equal to the one for S_2. Therefore, in the following, we only concentrate on the BEP analysis of S_1. For the instantaneous output signal-to-noise ratio (SNR) of $\hat{S}_1$, we find the following expression from (3a)

$$\gamma_\Sigma = \frac{R_1^2 R_2^2 + R_3^2 R_4^2 + 2R_1 R_2 R_3 R_4 \cos(\Theta_1 - \Theta_2 + \Theta_4 - \Theta_3)}{(R_2^2 + R_3^2) \cdot 2\sigma_n^2}, \tag{5}$$

where $2\sigma_n^2$ denotes the variance of the AWGN noise. It should be mentioned that if the channel is constant during the consecutive time slots t_1 and t_2, i.e., $H_{k1}(f', x_k, t_1) = H_{k1}(f', x_k, t_2)$ $(k = 1, 2)$, the instantaneous output SNR γ_Σ in (5) reduces to the one presented in [10, p. 214].

B. Statistical Properties of the Considered Channel Model

As shown in [5], the performance of an Alamouti coded OFDM system depends not only on the temporal correlation but also on the spatial correlation. For the purpose of performance analysis, we briefly review the main correlation functions of the considered channel, which is correlated in both spatial and temporal domains.

First, we consider the temporal ACF $r_{HH}(\tau)$ between the subchannels $H_{k1}(f', x_k, t_1)$ and $H_{k1}(f', x_k, t_2)$. By making use of the results in [11], we can express the temporal ACF $r_{HH}(\tau)$ as follows

$$\begin{aligned} r_{HH}(\tau) &= E\{H_{k1}^*(f', x_k, t_1) \cdot H_{k1}(f', x_k, t_2)\} \\ &= \sum_{\ell=1}^{\mathcal{L}} a_\ell^2 r_{\mu_\ell \mu_\ell}(\tau), \end{aligned} \tag{6}$$

where $\tau = t_2 - t_1$ and $r_{\mu_\ell \mu_\ell}(\tau)$ describes the temporal ACF between $\mu_\ell(x_k, t_1)$ and $\mu_\ell(x_k, t_2)$. Assuming isotropic scattering conditions, we have $r_{HH}(\tau) = 2\sigma_0^2 J_0(2\pi f_{\max}\tau)$. Here, $J_0(\cdot)$ is the zeroth-order Bessel function of the first kind and $f_{\max}$ represents the maximum Doppler frequency.

The space CCF $r_{HH}(\triangle x)$ between $H_{11}(f', x_1, t_i)$ and $H_{21}(f', x_2, t_i)$ can be computed via the definition $r_{HH}(\triangle x) = E\{H_{11}^*(f', x_1, t_i) \cdot H_{21}(f', x_2, t_i)\}$. Based on [11], we have

$$r_{HH}(\triangle x) = \sum_{\ell=1}^{\mathcal{L}} a_\ell^2 r_{\mu_\ell \mu_\ell}(\triangle x), \tag{7}$$

where $\triangle x = x_2 - x_1$. In (7), $r_{\mu_\ell \mu_\ell}(\triangle x)$ designates the space CCF of the random processes $\mu_\ell(x_1, t_i)$ and $\mu_\ell(x_2, t_i)$. For the case of isotropic scattering, we have $r_{HH}(\triangle x) = 2\sigma_0^2 J_0(2\pi \triangle x/\lambda)$, where λ denotes the wavelength.

$$\hat{S}_1 = [H_{11}(f', x_1, t_1)H_{11}^*(f', x_1, t_2) + H_{21}(f', x_2, t_1)H_{21}^*(f', x_2, t_2)]S_1 + H_{11}^*(f', x_1, t_2)N_1 + H_{21}(f', x_2, t_1)N_2^*, \tag{3a}$$

$$\hat{S}_2 = [H_{11}(f', x_1, t_1)H_{11}^*(f', x_1, t_2) + H_{21}(f', x_2, t_1)H_{21}^*(f', x_2, t_2)]S_2 + H_{21}^*(f', x_2, t_2)N_1 + H_{11}(f', x_1, t_1)N_2^*. \tag{3b}$$

The space-time CCF between $H_{11}(f', x_1, t_i)$ and $H_{21}(f', x_2, t_j)$ is defined as

$$r_{HH}(\triangle x, \tau) = E\{H_{11}^*(f', x_1, t_i) \cdot H_{21}(f', x_2, t_j)\}, \quad (8)$$

for $i, j = 1, 2$ and $i \neq j$. Finally, we mention that the space-time CCF $r_{HH}(\triangle x, \tau)$ can be represented by the sum of the space-time CCFs of different propagation paths weighted by the path power a_ℓ^2.

III. The BEP Performance of Alamouti Coded OFDM Systems over Fading Channels Correlated in Space and Time

In the following, we will first derive an analytical expression for the joint PDF of the envelopes R_1, R_2, R_3, and R_4, denoted by $p_{R_1R_2R_3R_4}(r_1, r_2, r_3, r_4)$. Thereafter, we will find a solution for the PDF of the instantaneous output SNR. At the end, the BEP can be easily derived by averaging the conditional BEP over the obtained PDF of the instantaneous output SNR [10].

A. The Derivation of the Joint PDF of Four Envelopes

We express the complex space-time-variant transfer functions by their real and imaginary parts in the following form

$$\begin{aligned} H_{11}(f', x_1, t_1) &= X_1 + jY_1, \quad H_{11}(f', x_1, t_2) = X_2 + jY_2, \\ H_{21}(f', x_2, t_1) &= X_3 + jY_3, \quad H_{21}(f', x_2, t_2) = X_4 + jY_4. \end{aligned} \quad (9)$$

As already mentioned in Section II, X_m and Y_n are independent Gaussian random variables $(m, n = 1, 2, 3, 4)$. Therefore, the joint PDF of the eight Gaussian random variables, i.e., X_1, X_2, X_3, X_4, Y_1, Y_2, Y_3, and Y_4, can be expressed by the product of two joint PDFs as follows

$$\begin{aligned} &p_{X_1X_2X_3X_4Y_1Y_2Y_3Y_4}(x_1, x_2, x_3, x_4, y_1, y_2, y_3, y_4) \quad (10) \\ &= p_{X_1X_2X_3X_4}(x_1, x_2, x_3, x_4) \cdot p_{Y_1Y_2Y_3Y_4}(y_1, y_2, y_3, y_4). \end{aligned}$$

Here, $p_{X_1X_2X_3X_4}(x_1, x_2, x_3, x_4)$ denotes the joint PDF of the variables X_1, X_2, X_3, and X_4, while the joint PDF of Y_1, Y_2, Y_3, and Y_4 is described by $p_{Y_1Y_2Y_3Y_4}(y_1, y_2, y_3, y_4)$.

Starting from the multivariate Gaussian distribution [12, Eq. (2.20)], we can compute the joint PDFs $p_{X_1X_2X_3X_4}(x_1, x_2, x_3, x_4)$ and $p_{Y_1Y_2Y_3Y_4}(y_1, y_2, y_3, y_4)$, which are presented at the bottom of this page [see (11) and (12)]. The symbols A, B, C, D, and E in (11) and (12) are given by

$$A = 2\rho_T\rho_x\rho_{x,T} + \sigma_0^2(\sigma_0^4 - \rho_T^2 - {\rho_x}^2 - \rho_{x,T}^2), \quad (13a)$$

$$B = 2\sigma_0^2\rho_x\rho_{x,T} - \rho_T(\sigma_0^4 - \rho_T^2 + {\rho_x}^2 + \rho_{x,T}^2), \quad (13b)$$

$$C = 2\sigma_0^2\rho_T\rho_{x,T} - \rho_x(\sigma_0^4 + \rho_T^2 - {\rho_x}^2 + \rho_{x,T}^2), \quad (13c)$$

$$D = 2\sigma_0^2\rho_T\rho_x - \rho_{x,T}(\sigma_0^4 + \rho_T^2 + {\rho_x}^2 - \rho_{x,T}^2), \quad (13d)$$

$$\begin{aligned} E = {} & (\sigma_0^4 - \rho_T^2)^2 + ({\rho_x}^2 - \rho_{x,T}^2)^2 \\ & - 2(\sigma_0^4 + \rho_T^2)({\rho_x}^2 + \rho_{x,T}^2) + 8\sigma_0^2\rho_T\rho_x\rho_{x,T}, \end{aligned} \quad (13e)$$

where $\rho_T = r_{HH}(T_s)/2$, $\rho_x = r_{HH}(\triangle x)/2$, and $\rho_{x,T} = r_{HH}(\triangle x, T_s)/2$.

Substituting (11) and (12) into (10), we obtain the analytical expression for the joint PDF $p_{X_1X_2X_3X_4Y_1Y_2Y_3Y_4}(x_1, x_2, x_3, x_4, y_1, y_2, y_3, y_4)$. Then, after transforming the Cartesian coordinates (x_m, y_m) into the polar coordinates (r_m, θ_m), we can express the joint PDF $p_{R_1R_2R_3R_4\Theta_1\Theta_2\Theta_3\Theta_4}(r_1, r_2, r_3, r_4, \theta_1, \theta_2, \theta_3, \theta_4)$ of the four envelopes $R_m = |X_m + jY_m|$ and the four phases $\Theta_m = \arg\{X_m + jY_m\}$ in the form shown at the bottom of this page [see (14)]. In this equation,

$$\begin{aligned} J = {} & \begin{vmatrix} \frac{\partial x_1}{\partial r_1} & \cdots & \frac{\partial x_1}{\partial r_4} & \frac{\partial x_1}{\partial \theta_1} & \cdots & \frac{\partial x_1}{\partial \theta_4} \\ \vdots & \ddots & \vdots & \vdots & \ddots & \vdots \\ \frac{\partial x_4}{\partial r_1} & \cdots & \frac{\partial x_4}{\partial r_4} & \frac{\partial x_4}{\partial \theta_1} & \cdots & \frac{\partial x_4}{\partial \theta_4} \\ \frac{\partial y_1}{\partial r_1} & \cdots & \frac{\partial y_1}{\partial r_4} & \frac{\partial y_1}{\partial \theta_1} & \cdots & \frac{\partial y_1}{\partial \theta_4} \\ \vdots & \ddots & \vdots & \vdots & \ddots & \vdots \\ \frac{\partial y_4}{\partial r_1} & \cdots & \frac{\partial y_4}{\partial r_4} & \frac{\partial y_4}{\partial \theta_1} & \cdots & \frac{\partial y_4}{\partial \theta_4} \end{vmatrix} \\ = {} & r_1r_2r_3r_4 \end{aligned} \quad (15)$$

denotes the Jacobian determinant. Now, the joint PDF $p_{R_1R_2R_3R_4}(r_1, r_2, r_3, r_4)$ of the envelopes R_1, R_2, R_3, and R_4

$$p_{X_1X_2X_3X_4}(x_1, x_2, x_3, x_4) = \frac{1}{(2\pi)^2\sqrt{E}} e^{-\frac{1}{2E}[A(x_1^2+x_2^2+x_3^2+x_4^2)+B(x_1x_2+x_3x_4)+C(x_1x_3+x_2x_4)+D(x_1x_4+x_2x_3)]}, \quad (11)$$

$$p_{Y_1Y_2Y_3Y_4}(y_1, y_2, y_3, y_4) = \frac{1}{(2\pi)^2\sqrt{E}} e^{-\frac{1}{2E}[A(y_1^2+y_2^2+y_3^2+y_4^2)+B(y_1y_2+y_3y_4)+C(y_1y_3+y_2y_4)+D(y_1y_4+y_2y_3)]}. \quad (12)$$

$$\begin{aligned} &p_{R_1R_2R_3R_4\Theta_1\Theta_2\Theta_3\Theta_4}(r_1, r_2, r_3, r_4, \theta_1, \theta_2, \theta_3, \theta_4) \\ &= |J| \cdot p_{X_1X_2X_3X_4Y_1Y_2Y_3Y_4}(r_1\cos\theta_1, r_2\cos\theta_2, r_3\cos\theta_3, r_4\cos\theta_4, r_1\sin\theta_1, r_2\sin\theta_2, r_3\sin\theta_3, r_4\sin\theta_4), \end{aligned} \quad (14)$$

$$\begin{aligned} p_{R_1R_2R_3R_4}(r_1, r_2, r_3, r_4) = {} & \frac{r_1r_2r_3r_4}{(2\pi)^2E} \cdot e^{[-\frac{A}{2E}(r_1^2+r_2^2+r_3^2+r_4^2)]} \int_0^{2\pi}\int_0^{2\pi} e^{-\frac{1}{E}[Br_3r_4\cos(\varphi_2)+Cr_2r_4\cos(\varphi_1+\varphi_2)+Dr_2r_3\cos(\varphi_1)]} \\ & I_0\left(\frac{1}{E}\sqrt{B^2r_1^2r_2^2 + C^2r_1^2r_3^2 + D^2r_1^2r_4^2 + 2r_1r_2r_3r_4[BC\cos(\varphi_1) + BD\cos(\varphi_1+\varphi_2) + CD\cos(\varphi_2)]}\right) d\varphi_1 d\varphi_2. \end{aligned} \quad (16)$$

can be computed by integrating (14) over the phases θ_1, θ_2, θ_3, and θ_4, which results finally in the form presented at the bottom of this page [see (16)].

B. Derivation of the PDF of the Output Instantaneous SNR

This subsection is devoted to find an expression for the PDF $p_{\gamma_\Sigma}(\gamma)$ of the instantaneous output SNR. It is shown in (5) that the instantaneous output SNR is determined by the envelopes (R_1, R_2, R_3, R_4) and the phases (Θ_1, Θ_2, Θ_3, Θ_4). Even if the joint probability density function (PDF) of the envelopes and phases is known in advance, it is mathematically complicated to find the theoretical expression for the PDF of the instantaneous output SNR.

For the purpose of performance analysis, we introduce an approximation for the instantaneous output SNR by neglecting the difference between the phase changes $\Theta_1 - \Theta_2$ and $\Theta_3 - \Theta_4$, i.e., $\Theta_1 - \Theta_2 - (\Theta_3 - \Theta_4) \approx 0$. Thus, the instantaneous output SNR γ_Σ in (5) can be approximated as

$$\gamma_\Sigma \approx \frac{R_1^2 R_2^2 + R_3^2 R_4^2 + 2R_1 R_2 R_3 R_4}{(R_2^2 + R_3^2) \cdot 2\sigma_n^2}. \tag{17}$$

To verify its accuracy, we compare the PDF of the exact instantaneous output SNR with that of the approximate one by means of simulations. Figure 1 presents the simulation results for both PDFs by considering different types of correlated channels, including (i) channels correlated in time, (ii) channels correlated in space, and (iii) channels correlated in both domains. All simulation results presented in Fig. 1 are obtained by considering a typical 6-path rural area propagation scenario [13]. It is assumed that the average SNR $\bar{\gamma}$ is 5 dB, the symbol duration T_s equals 6.4 μs, the maximum Doppler frequency $f_{\max}$ is 500 Hz, and the normalized transmit antenna spacing $\triangle x/\lambda$ is 0.5.

As illustrated in Fig. 1, the difference between the two types of PDFs is indistinguishable. This means that the PDF of the approximate instantaneous output SNR is almost equivalent to that of the exact instantaneous output SNR. Thus, the overall phase contribution to the instantaneous output SNR is negligible. It should be emphasized again that we have not neglected the phase difference between Θ_1 and Θ_2 (or between Θ_3 and Θ_4), i.e., $\Theta_1 \neq \Theta_2$ and $\Theta_3 \neq \Theta_4$. Instead of this, we only assume that $(\Theta_1 - \Theta_2) - (\Theta_3 - \Theta_4) \approx 0$. The accuracy of such an approximation has been confirmed by the excellent fitting between the PDF curves in Fig. 1.

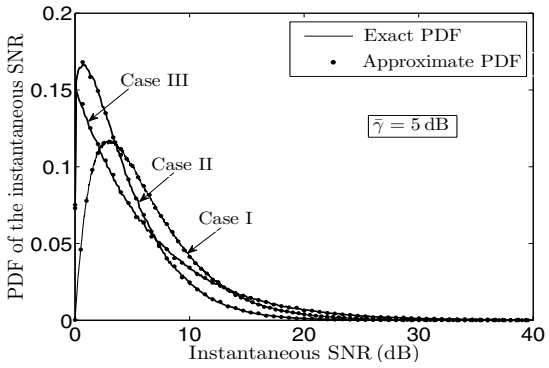

Fig. 1. Simulation results for the PDF of the instantaneous output SNR for channels correlated in time (case I), channels correlated in space (case II), and channels correlated in space and time (case III).

To obtain the PDF of the instantaneous output SNR, we start from deriving the PDF of the random variable Z defined by

$$Z = \frac{R_1^2 R_2^2 + R_3^2 R_4^2 + 2R_1 R_2 R_3 R_4}{R_2^2 + R_3^2}. \tag{18}$$

Let us define a system of equations as follows

$$z_1 = (r_1 r_2 + r_3 r_4)^2,\ z_2 = r_2^2 + r_3^2,\ z_3 = r_1 r_2,\ z_4 = r_3^2, \tag{19}$$

from which we find the following real-valued solutions under the preconditions $z_3 < \sqrt{z_1}$ and $z_4 < z_2$

$$r_1 = \frac{z_3}{\sqrt{z_2 - z_4}},\ r_2 = \sqrt{z_2 - z_4},\ r_3 = \sqrt{z_4},\ r_4 = \frac{\sqrt{z_1} - z_3}{\sqrt{z_4}}. \tag{20}$$

With the concept of transformation of random variables [14], we can express the join PDF of the random variables Z_1, Z_2, Z_3, and Z_4 as follows

$$p_{Z_1 Z_2 Z_3 Z_4}(z_1, z_2, z_3, z_4) = |J(z_1, z_2, z_3, z_4)| \cdot p_{R_1 R_2 R_3 R_4}\left(\frac{z_3}{\sqrt{z_2 - z_4}}, \sqrt{z_2 - z_4}, \sqrt{z_4}, \frac{\sqrt{z_1} - z_3}{\sqrt{z_4}}\right), \tag{21}$$

where the Jacobian determinant $J(z_1, z_2, z_3, z_4)$ equals $-1/[8\sqrt{z_1} z_4 (z_2 - z_4)]$. Then, integrating the joint PDF $p_{Z_1 Z_2 Z_3 Z_4}(z_1, z_2, z_3, z_4)$ over z_3 and z_4 results in the joint PDF of the random variables Z_1 and Z_2, i.e.,

$$p_{Z_1 Z_2}(z_1, z_2) = \frac{1}{8\sqrt{z_1}} \int_0^{\sqrt{z_1}} \int_0^{z_2} \frac{1}{z_4 (z_2 - z_4)} \cdot p_{R_1 R_2 R_3 R_4}\left(\frac{z_3}{\sqrt{z_2 - z_4}}, \sqrt{z_2 - z_4}, \sqrt{z_4}, \frac{\sqrt{z_1} - z_3}{\sqrt{z_4}}\right) dz_4 dz_3. \tag{22}$$

Applying the rule presented in [14, Eq. (6–59)], we obtain the following expression for the PDF of the random variable $Z = Z_1/Z_2$

$$p_Z(z) = \frac{1}{8} \int_0^{\infty} \int_0^{\sqrt{z z_2}} \int_0^{z_2} \frac{z_2}{z_4 (z_2 - z_4) \sqrt{z z_2}} \cdot p_{R_1 R_2 R_3 R_4}\left(\frac{z_3}{\sqrt{z_2 - z_4}}, \sqrt{z_2 - z_4}, \sqrt{z_4}, \frac{\sqrt{z z_2} - z_3}{\sqrt{z_4}}\right) dz_4 dz_3 dz_2. \tag{23}$$

With [14, Eq. (5–3)], we can now express the desired PDF $p_{\gamma_\Sigma}(\gamma)$ of $\gamma_\Sigma = Z/2\sigma_n^2$ in terms of the joint PDF $p_{R_1 R_2 R_3 R_4}(r_1, r_2, r_3, r_4)$ as follows

$$p_{\gamma_\Sigma}(\gamma) = \frac{2\sigma_0^2}{8\bar{\gamma}} \int_0^{\infty} \int_0^{w} \int_0^{z_2} \frac{z_2}{z_4 (z_2 - z_4) w} \cdot p_{R_1 R_2 R_3 R_4}\left(\frac{z_3}{\sqrt{z_2 - z_4}}, \sqrt{z_2 - z_4}, \sqrt{z_4}, \frac{w - z_3}{\sqrt{z_4}}\right) dz_4 dz_3 dz_2, \tag{24}$$

where the upper limit w in the second integral represents $w = \sqrt{2\sigma_0^2 \gamma z_2/\bar{\gamma}}$.

C. Expression for the BEP

The BEP of the Alamouti coded OFDM system can be calculated by means of the relation [10, Eq. (7.20)]

$$P_b = \int_0^\infty p_{\gamma_\Sigma}(\gamma) \cdot P_{b|\gamma_\Sigma}(\gamma)\, d\gamma, \tag{25}$$

where $P_{b|\gamma_\Sigma}(\gamma)$ is the conditional BEP of a digital modulation scheme for a specific value of the SNR γ. For the binary phase-shift keying (BPSK) modulation scheme, e.g., $P_{b|\gamma_\Sigma}(\gamma) = \mathrm{erfc}(\sqrt{\gamma})/2$. Here, $\mathrm{erfc}(x) = \int_x^\infty \frac{2}{\sqrt{\pi}} e^{-y^2} dy$ represents the complementary error function.

Substituting the derived joint PDF $p_{\gamma_\Sigma}(\gamma)$ [see (24)] into (25) and taking (16) into account, we finally come to the result of the BEP of a BPSK Alamouti coded OFDM system as shown in (26).

In the following, we will discuss two special cases. By considering $\rho_x = 0$ and $\rho_{x,_T} = 0$, the BEP in (26) reduces to the BEP

$$\begin{aligned} P_b = {} & \frac{2\sigma_0^2}{16(\sigma_0^4 - \rho_{_T}^2)^2 \bar{\gamma}} \int_0^\infty \int_0^\infty \int_0^w \int_0^{z_2} \frac{z_2 z_3 (w - z_3)}{z_4 (z_2 - z_4) w} \\ & \cdot e^{-\frac{\sigma_0^2}{2(\sigma_0^4 - \rho_{_T}^2)} \left[\frac{(w-z_3)^2}{z_4} + z_2 + \frac{z_3^2}{z_2 - z_4}\right]} \cdot \mathrm{erfc}(\sqrt{\gamma}) \\ & \cdot I_0\left(\frac{z_3 \rho_{_T}}{\sigma_0^4 - \rho_{_T}^2}\right) I_0\left(\frac{(w - z_3)\rho_{_T}}{\sigma_0^4 - \rho_{_T}^2}\right) dz_4 dz_3 dz_2 d\gamma, \end{aligned} \tag{27}$$

which has been presented in [7, Eq. (11)] describing the system performance over fading channels correlated in time.

For the case when $\rho_{_T} = 0$ and $\rho_{x,_T} = 0$, the BEP in (26) can be reduced to the result presented in [7, Eq. (15)]

$$\begin{aligned} P_b = {} & \frac{2\sigma_0^2}{16(\sigma_0^4 - \rho_x^2)^2 \bar{\gamma}} \int_0^\infty \int_0^\infty \int_0^w \int_0^{z_2} \frac{z_2 z_3 (w - z_3)}{z_4 (z_2 - z_4) w} \\ & \cdot I_0\left(\frac{z_3 \sqrt{z_4} \rho_x}{(\sigma_0^4 - \rho_x^2)\sqrt{z_2 - z_4}}\right) I_0\left(\frac{(w - z_3)\sqrt{z_2 - z_4}\rho_x}{(\sigma_0^4 - \rho_x^2)\sqrt{z_4}}\right) \\ & \cdot e^{-\frac{\sigma_0^2}{2(\sigma_0^4 - \rho_x^2)} \left[\frac{(w-z_3)^2}{z_4} + z_2 + \frac{z_3^2}{z_2 - z_4}\right]} \cdot \mathrm{erfc}(\sqrt{\gamma}) dz_4 dz_3 dz_2 d\gamma, \end{aligned} \tag{28}$$

which represents the BEP performance of the Alamouti coded OFDM system over fading channels correlated in space.

IV. Numerical Results

This section is devoted to illustrate the theoretical BEP results given by (26), (27), and (28). To confirm their correctness, all derived theoretical results will be validated by system simulations. In all the simulations, we assume that the considered OFDM system consists of $K = 64$ subcarriers. All other parameters are the same as in Section II.

The BEP performance over fading channels correlated in spatial and temporal domains is presented in Fig. 2 for different antenna spacings $\triangle x$ and different maximum Doppler frequencies $f_{\max}$. It is shown that the theoretical BEPs calculated by (26) match perfectly the ones obtained by system simulations. Moreover, we can observe that both the antenna spacing and the maximum Doppler frequency have an impact on the system performance.

In the following two figures, we present the BEP performance for the two special cases, where the channels are correlated either in the temporal or spatial domain. Figure 3 illustrates the BEP over channels correlated in the temporal domain for $f_{\max} = 100\,\mathrm{Hz}$ and $f_{\max} = 500\,\mathrm{Hz}$ [see (27)]. This figure also presents the relevant simulation results, which again confirm the correctness of the analytical ones. It turns out that the maximum Doppler frequency has an influence on the system performance, which can be attributed to the channel variations during two consecutive transmission time slots. The performance degrades when changing the maximum Doppler frequency $f_{\max}$ from $100\,\mathrm{Hz}$ to $500\,\mathrm{Hz}$.

The theoretical results of the BEP described by (28) are

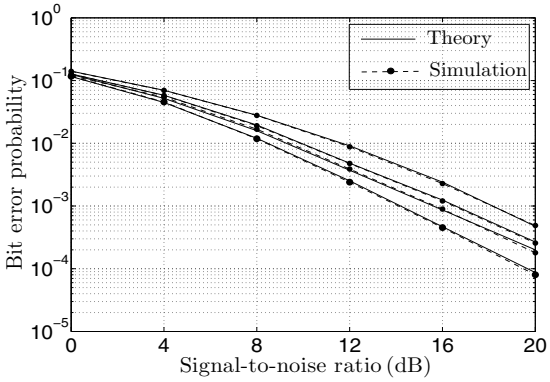

Fig. 2. BEP performance of Alamouti coded OFDM systems over fading channels correlated in space and time for different values of the maximum Doppler frequency $f_{\max}$ and the antenna spacing $\triangle x$.

$$\begin{aligned} P_b = {} & \frac{2\sigma_0^2}{64\pi^2 \bar{\gamma} E} \int_0^\infty \int_0^\infty \int_0^w \int_0^{z_2} \frac{z_2 z_3 (w - z_3)}{z_4 (z_2 - z_4) w} \cdot e^{-\frac{A}{2E}\left[\frac{(w-z_3)^2}{z_4} + z_2 + \frac{z_3^2}{z_2 - z_4}\right]} \cdot \mathrm{erfc}(\sqrt{\gamma}) \\ & \cdot \int_0^{2\pi} \int_0^{2\pi} I_0\left(\frac{1}{E}\sqrt{B^2 z_3^2 + C^2 \frac{z_4 z_3^2}{z_2 - z_4} + D^2 \frac{z_3^2 (w - z_3)^2}{z_4 (z_2 - z_4)} + 2 z_3 (w - z_3)[BC\cos\varphi_1 + BD\cos(\varphi_1 + \varphi_2) + CD\cos\varphi_1]}\right) \\ & \cdot e^{-\frac{1}{E}[B(w-z_3)\cos\varphi_2 + C(w-z_3)\sqrt{\frac{(z_2 - z_4)}{z_4}}\cos(\varphi_1 + \varphi_2) + D\sqrt{z_4(z_2 - z_4)}\cos\varphi_1]} d\varphi_1 d\varphi_2 dz_4 dz_3 dz_2 d\gamma, \end{aligned} \tag{26}$$

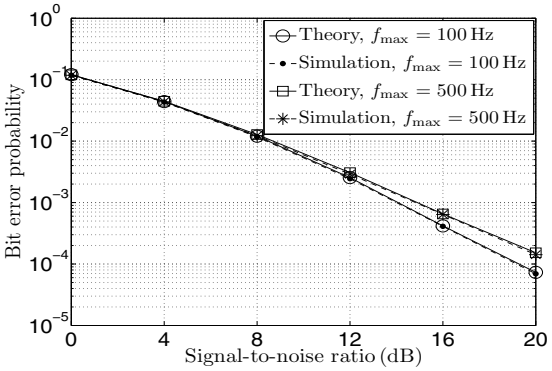

Fig. 3. BEP performance of Alamouti coded OFDM systems over fading channels correlated in time for $f_{\max} = 100\,\mathrm{Hz}$ and $f_{\max} = 500\,\mathrm{Hz}$.

depicted in Fig. 4 for different antenna spacings $\triangle x = 0.1\lambda$ and $\triangle x = 3\lambda$. It can be concluded from Fig. 4 that the system performance can be improved by increasing the antenna spacing. This can be explained by the fact that the spatial correlation between subchannels becomes smaller when the antenna spacing increases. By comparing Fig. 3 with Fig. 4, we may conclude that though the temporal ACF and the space CCF have the same shape, their influence on the system performance is inverse.

V. Conclusion

In this paper, we have analyzed the performance of Alamouti coded OFDM systems over multipath Rayleigh fading channels correlated in space and time. In our analysis, we have considered the physically more realistic case that the channel envelope changes during two consecutive transmission time slots. It has been shown by simulations that the instantaneous output SNR strongly depends on the statistics of the envelopes of the space-time-variant transfer functions, while the impact of the overall random phase contribution is negligible. An analytical expression has been derived for the BEP of an Alamouti coded OFDM system over fading channels correlated both in temporal and spatial domains. The derived BEP includes the known BEPs for channels correlated in the temporal or spatial domain as special cases.

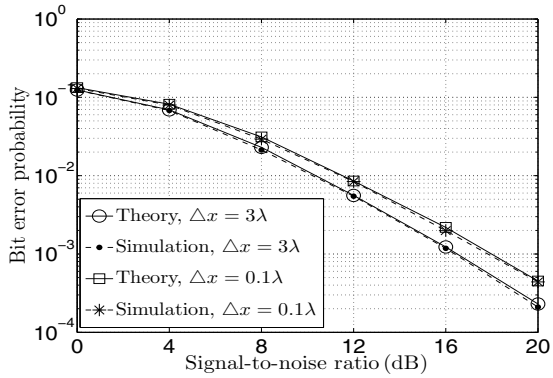

Fig. 4. BEP performance of Alamouti coded OFDM systems over fading channels correlated in space for $\triangle x = 0.1\lambda$ and $\triangle x = 3\lambda$.

With the help of the derived BEP expressions, we have numerically evaluated the BEP performance for different types of correlated channels, where the impact of the maximum Doppler frequency and the antenna spacing on the system performance has been discussed. We found that the system performance deteriorates when increasing the maximum Doppler frequency due to a lower temporal ACF. In contrast, the performance improves if increasing the antenna spacing due to a lower space CCF. Therefore, it can be concluded that the temporal ACF and the space CCF have inverse effect on the system performance though they have the same shape under isotropic scattering conditions. In addition, we have confirmed all the theoretical results by system simulations.

References

[1] V. Tarokh, N. Seshadri, and A. R. Calderbank, "Space-time codes for high data rate wireless communication: Performance criterion and code construction," *IEEE Trans. Inf. Theory*, vol. 44, no. 2, pp. 744–765, Mar. 1998.

[2] S. M. Alamouti, "A simple transmit diversity technique for wireless communications," *IEEE Journal on Selected Areas in Commun.*, vol. 16, no. 8, pp. 1451–1458, Oct. 1998.

[3] V. Tarokh, H. Jafarkhani, and A. R. Calderbank, "Space-time block coding for wireless communications: Performance results," *IEEE Journal on Selected Areas in Commun.*, vol. 17, no. 3, pp. 451–460, Mar. 1999.

[4] D. B. Lin, P. H. Chiang, and H. J. Li, "Performance analysis of two–branch transmit diversity block–coded OFDM systems in time–varying multipath Rayleigh–fading channels," *IEEE Trans. on Veh. Technol.*, vol. 54, no. 1, pp. 136–148, Jan. 2005.

[5] Y. Ma and M. Pätzold, "Performance comparison of space-time coded MIMO-OFDM systems using different wideband MIMO channel models," in *Proc. 4th IEEE International Symposium on Wireless Communication Systems, ISWCS 2007*. Trondheim, Norway, Dec. 2007, pp. 762–766.

[6] E. Ko and D. Hong, "A robust transmit diversity for OFDM systems in spatially correlated Rayleigh fading channels," in *Proc. 59th Vehicular Technology Conference, VTC 2004-Spring*, vol. 4. Milan, Italy, May 2004, pp. 1840–1843.

[7] Y. Ma and M. Pätzold, "Performance analysis of STBC-OFDM systems in temporally or spatially correlated fading channels," in *Proc. IEEE Wireless Communication and Network Conference, WCNC 2010*. Australia, Apr. 2010, accepted for publication.

[8] A. Vielmon, Y. Li, and J. R. Barry, "Performance of Alamouti transmit diversity over time–varying Rayleigh–fading channels," *IEEE Trans. on Wire. Commun.*, vol. 3, no. 5, pp. 1369–1373, Sept. 2004.

[9] G. Abreu and R. Kohno, "Non-differential space-time transmission diversity in fast fading," in *Proc. 13th IEEE International Symposium on Personal, Indoor and Mobile Radio Communications*, vol. 1. Lisbon, Portugal, Sept. 2002, pp. 74–78.

[10] A. Goldsmith, *Wireless Communications*. Cambridge University Press, 2005.

[11] M. Pätzold, "System functions and characteristic quantities of spatial deterministic Gaussian uncorrelated scattering processes," in *Proc. 57th IEEE Vehicular Technology Conference, VTC 2003-Spring*, vol. 1. Jeju, Korea, Apr. 2003, pp. 256–2611.

[12] ——, *Mobile Fading Channels*. Chichester: John Wiley & Sons, 2002.

[13] COST 207, *Digital land mobile radio communications*. Office for Official Publications of the European Communities, Final report, Luxembourg, 1989.

[14] A. Papoulis and S. U. Pillai, *Probability, Random Variables and Stochastic Processes*. New York: McGraw-Hill, 4th edition, 2002.